Revisiting the Blackfoot 3C-2D broad-band seismic data

Han-xing Lu and Rolf Maier

ABSTRACT

Four lines of 2D vertical and three-component seismic data were acquired in the Blackfoot area east of Calgary in July, 1995. The data were sorted by the frequencies of the 3C geophones, processed, and stacked. The influence of the frequency is shown by focusing on a target zone. Both vertical and radial component data were processed, but only results for vertical component data are presented because of the low resolution of the radial component data.

INTRODUCTION

A broad-band seismic survey was conducted by CREWES over the Blackfoot Field east of Calgary, which is owned and operated by Encana (formerly PanCanadian Petroleum Ltd.), in July of 1995. Details of the location, geometry, and instrumentation of the survey may be found in Gallant (1995). This 3C-2D line was 4 km long; the receiver interval was 20 m, and shots of 6 kg were placed between receiver stations at a depth of 18 m.

Four types of geophones were used in this survey: On the first line, 200 10 Hz vertical geophones were planted; these geophones were in strings of 6 per station, planted as two parallel sets of three geophones. One meter from the first line, a second line with 10 Hz 3-C geophones was deployed, with a total of 600 channels deployed with three cables, one per component. A third line of 600 channels of 4.5 Hz geophones was deployed in this survey. The fourth line consisted of 200 2 Hz vertical geophones. Only 60 horizontal (inline) 2 Hz geophones were available. Details on the geophones and other components are listed in Gallant (1995); several more reports dealing with these data may be found in the same location.

These data were reprocessed by the first author because they are still of interest for student research projects. The results are only partly as one might expect, as will be shown in the following section.

RESULTS

The three vertical component data sets (2 Hz, 4.5 Hz, 10 Hz), and the single-component 10 Hz string geophone data, were processed by conventional processing procedures. None of the stacked sections have an AGC or band-pass applied. The differences in the target zone are quite striking; in the 2 Hz case the event at 1080 ms shows a stronger discontinuity at lower frequencies.

Only stacked sections for the vertical component data of the four types of geophones are presented here. Sections for the horizontal components are not shown because the resolution was too low to provide good results.

Figures 1 to 3 show the results for the 3-C 2 Hz, 4.5 Hz, and 10 Hz geophones, respectively; figure 4 shows the result for the vertical-component-only geophone. The differences show trends for the two ends of the target event depending on the frequency of the geophone.

In these plots the left-hand side of the target event becomes more focused in the higher frequency data, and can be seen to pinch out as it approaches the larger event from below. On the right-hand side there is an abrupt change in character and elevation of the event the target seems to be a part of, which is more clearly expressed in the low-frequency geophone data. Having more low frequencies seems to make for a clearer demarcation of the target event.

The left-hand side of the plot shows a slow approach of two events; interestingly, the low-frequency geophone data seem to decrease the distinction between the two events. The vertical component only geophone seems to give slightly more crisp events than the corresponding 10 Hz vertical component data. The reason for this is unknown.

Figure 5 highlights the differences in the target zone between different sections by removing some of the surrounding data. The caption indicates which case each panel refers to. It shows only the data in the red boxes and allows for an easy comparison between related parts of different sections.

Figure 6 shows migrated versions of the structure stacks shown in figure 5. Besides some noise removal the observations to be made parallel those for the structure stacks: the left-hand side of the target gets more diffuse as some low frequencies are lost while the right-hand side of the event gains in clarity.

Figure 7 shows part of a representative shot for each kind of geophones, with the target zone framed in a blue box. The central panels show a zoomed version of the data in the blue box, the right-hand panels show the Fourier spectrum of the data in the box. The slope of the amplitude spectrum from zero to about 15 Hz is clearly steeper in the high-frequency geophone case, as would be expected. The fact that the remainders of the spectra are almost identical lends credence to this observation. Hence, low-frequency geophones not only provide a larger range of frequencies but also show more sensitivity to low frequencies in general.

Figure 8 shows the same kinds of data as figure 7 for the poststack Kirchhoff time migrated equivalents of the data in figure 7. The spectra are surprising: not only do the higher frequency portions vary considerably, but the low-frequency portion is stronger for the high-frequency geophones. This is a rather unexpected artifact of the migration algorithm. The migrated section is partly smoothed by the migration, but the effect is much exaggerated by the low resolution of screens, hence the marked difference between the last two panels.

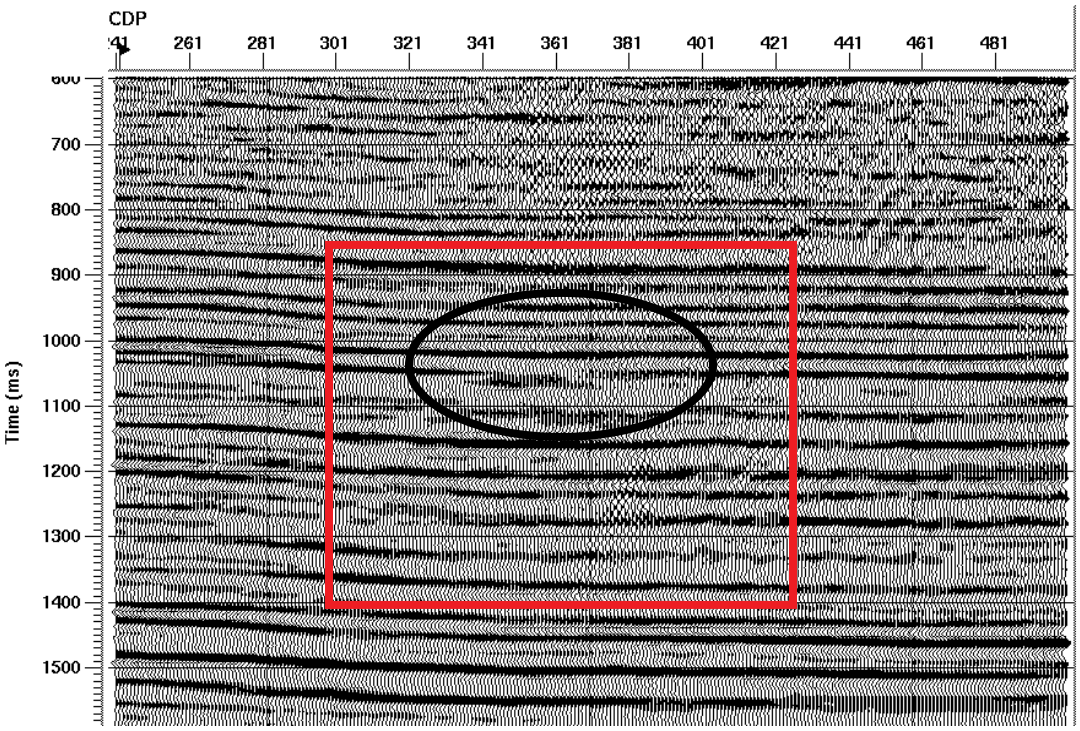

FIG. 1. Stacked section of the vertical component from 2 Hz 3-C geophones. The target zone (reservoir) is in the ellipse.

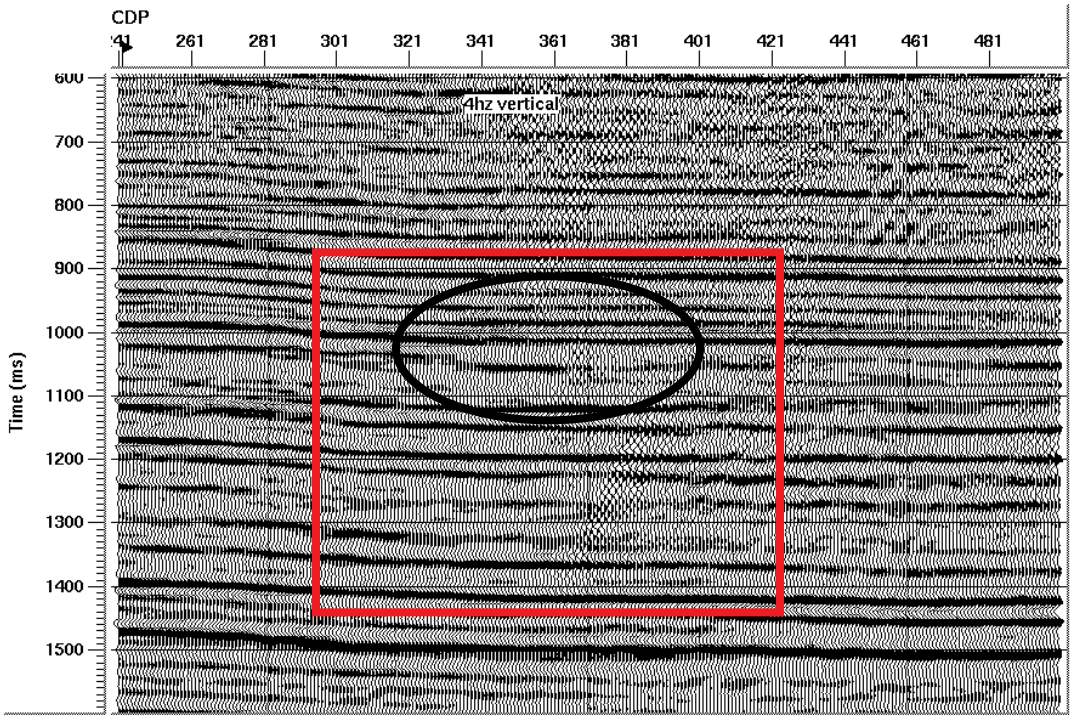

FIG. 2. Stacked section of the vertical component from 4 Hz 3-C geophones. The target zone (reservoir) is in the ellipse.

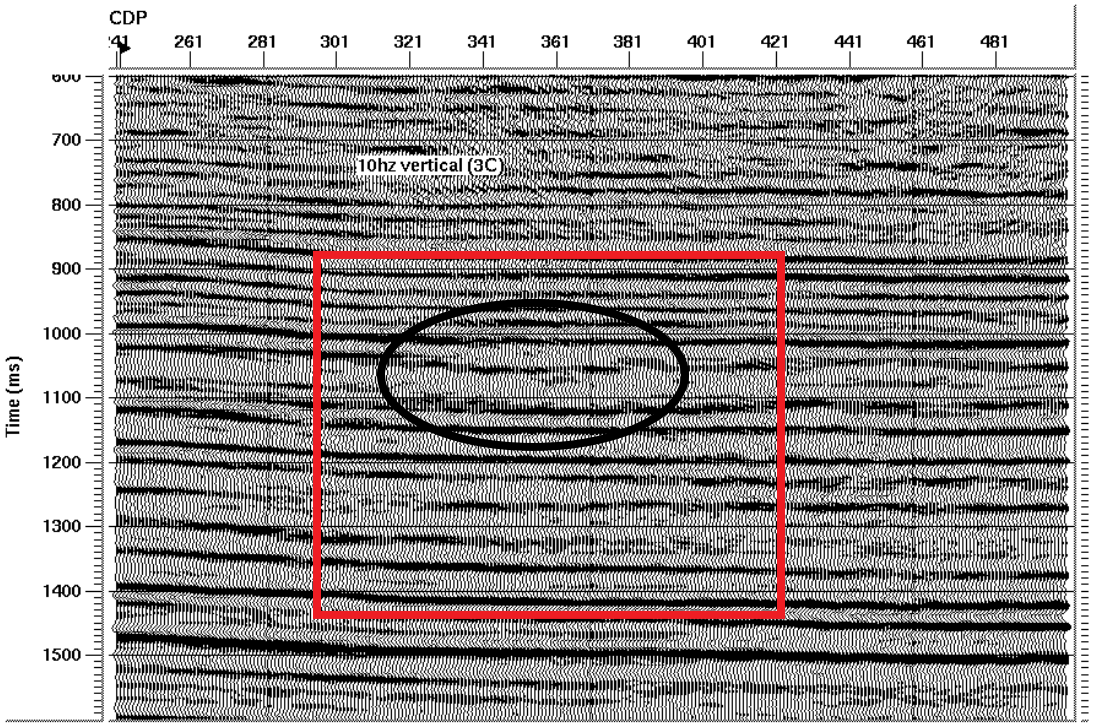

FIG. 3. Stacked section of the vertical component from 10 Hz 3-C geophones.

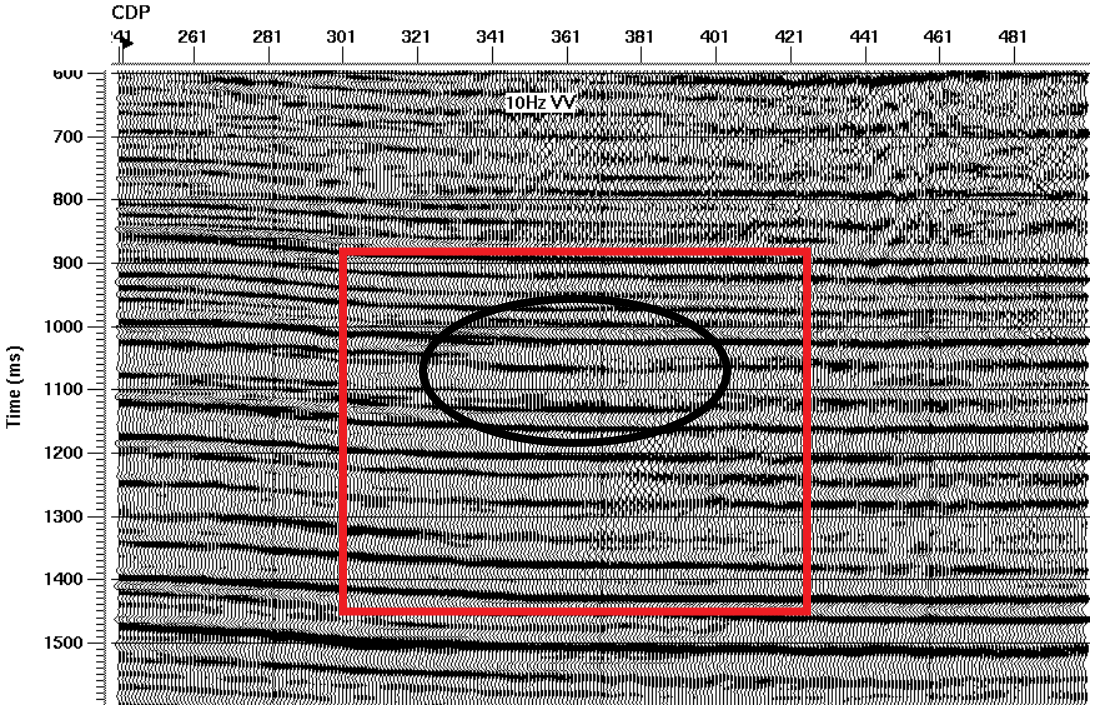

FIG. 4. Stacked section from 10 Hz vertical component only string geophones. The target zone (reservoir) is in the ellipse.

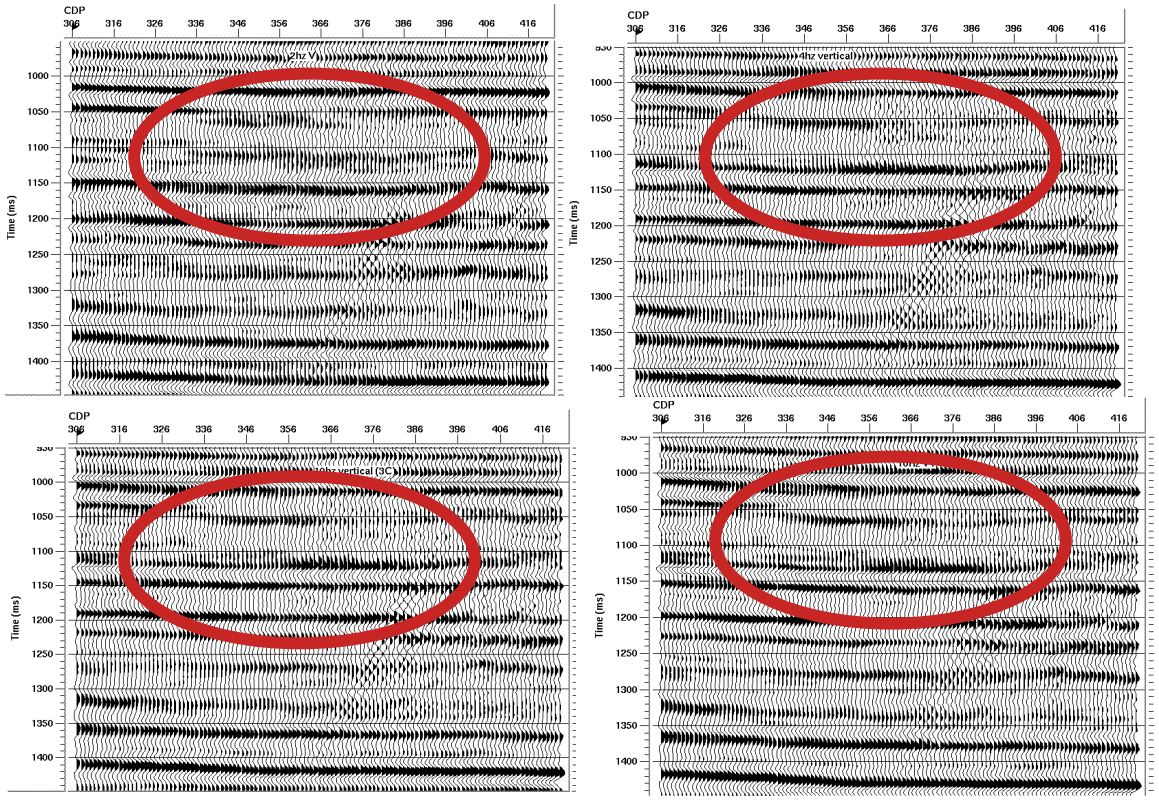

FIG. 5. Stacked sections of the vertical component from 2 Hz (top-left), 4.5 Hz (top-right); 10 Hz from 3C (bottom-left) and 10 Hz string geophones (bottom-right).

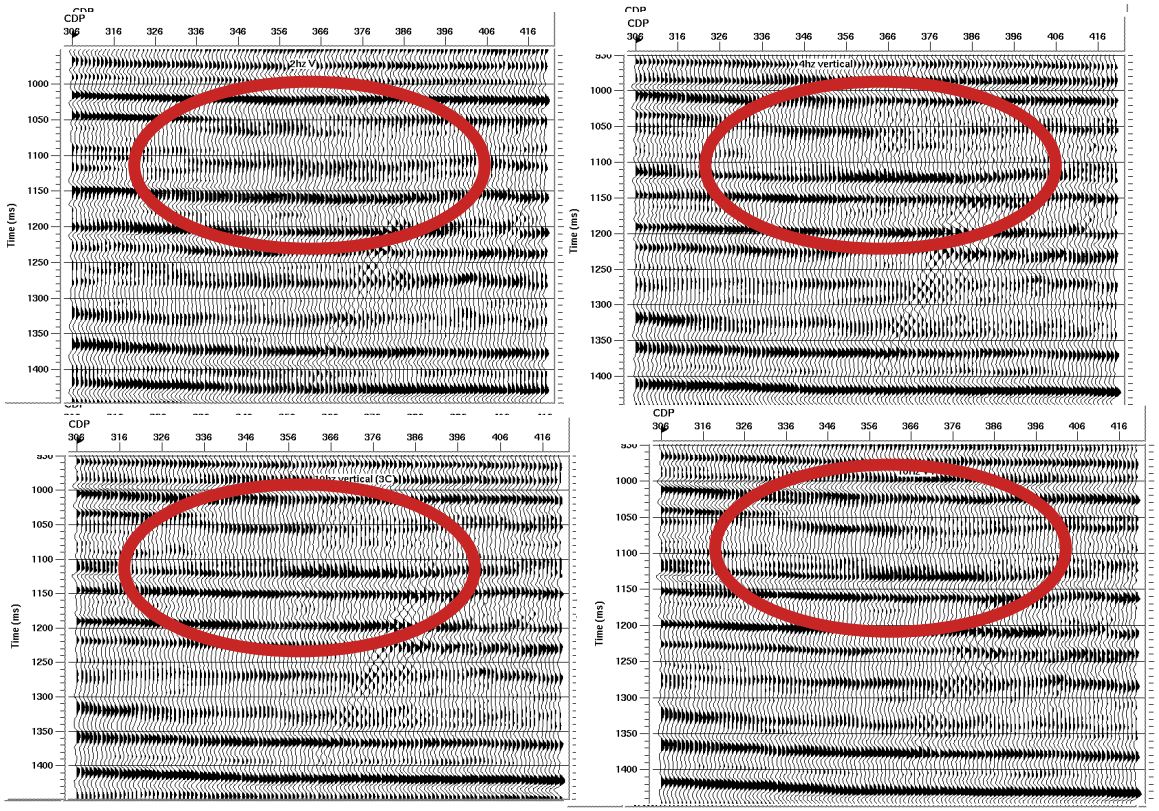

FIG. 6. Migrated sections of the vertical component from 2 Hz (top-left), 4.5 Hz (top-right); 10 Hz from 3-C (bottom-left) and 10 Hz string geophones (bottom-right).

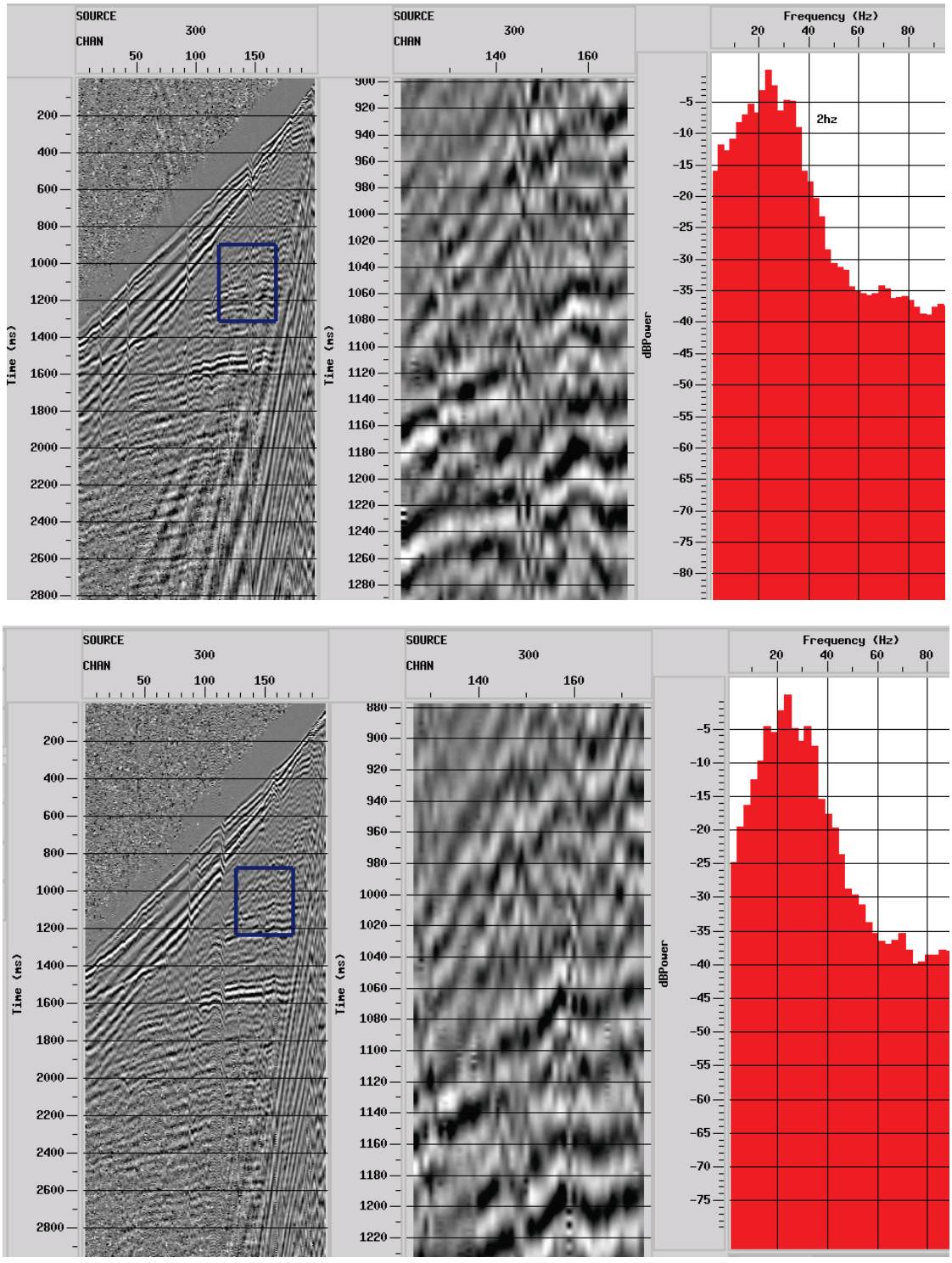

FIG. 7. Spectral analysis for shot gathers of 2 Hz 3-C geophones (top); for 10 Hz 3-C phones (centre), and the zoomed in spectra (bottom).

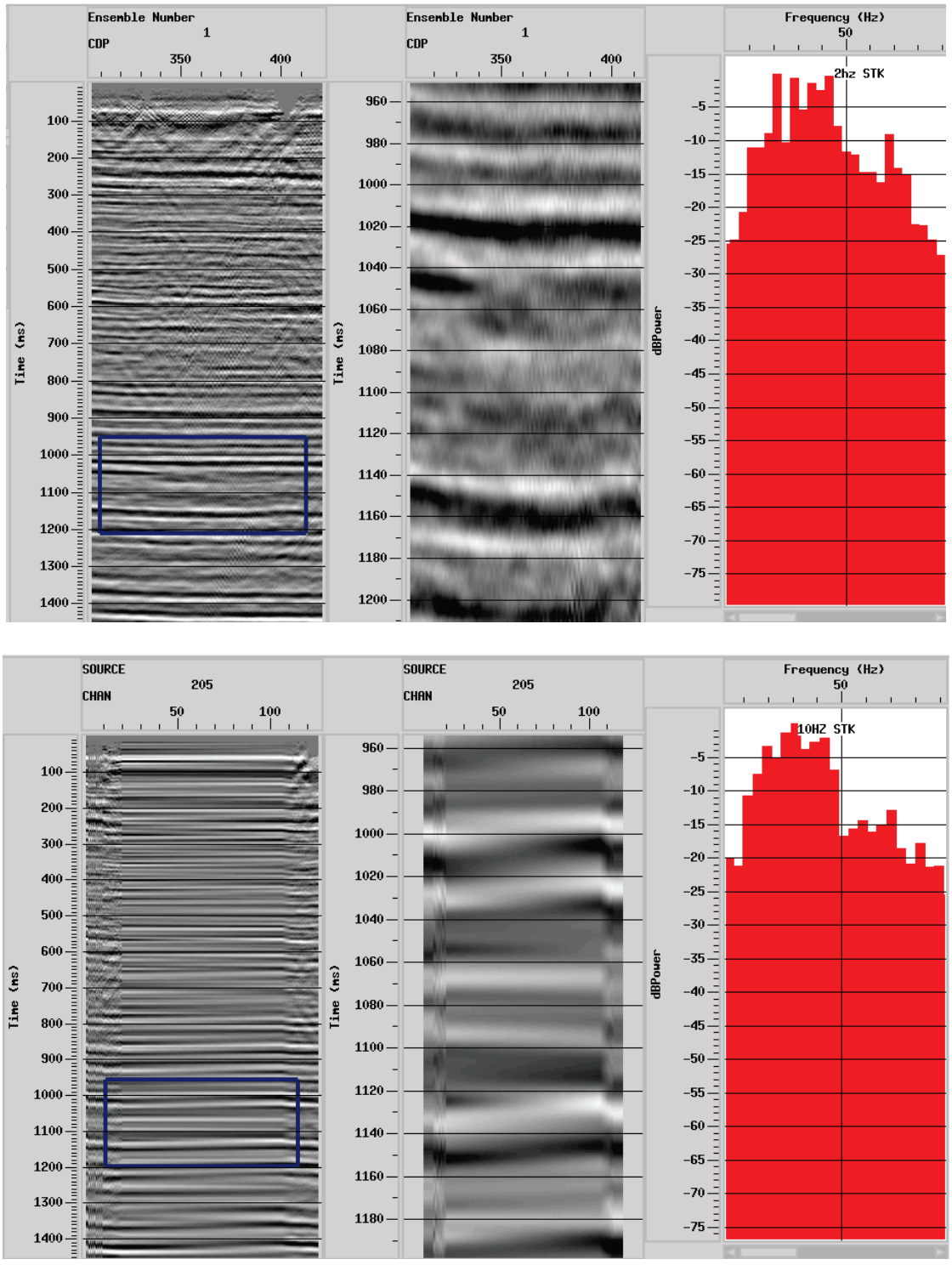

FIG. 8. Spectra for the structure stack of 2 Hz 3-C data (top), and for 10 Hz 3-C data (bottom).

ACKOWLEDGEMENT

We would like to thank former PanCanadian Ltd. (EnCana now) for permitting the acquisition. Detailed acknowledgements are given in the reference. We also like to thank Landmark and Hampson-Russel for donating ProMAX and GLI3D. Finally we thank the CREWES sponsors for their continued support which enables us to run such experiments, and our colleagues for their help.

CONCLUSION

The data show low-frequency geophones to boost the range of low frequencies. Having them does not always seem to be a boon. While some features get better resolved with the added frequencies, others suffer even if they are part of the same event. Whether the apparent loss of signal in the case of the low frequency geophones corresponds to a real loss of data or only the removal of an artifact is a point only an interpreter familiar with data of the area can decide.

REFERENCE

Gallant, E. V., Stewart, R. R., Bertram, M. B., and Lawton, D. C., 1995, Acquisition of the Blackfoot broad-band seismic survey: CREWES Research Report, **7**, 36.1-36.9.